J. Fluid Mech. (1967), *vol.* 29, *part* 4, *pp.* 745–763
Printed in Great Britain

Boundary-layer instability experiment with localized disturbance

By B. R. VASUDEVA

Department of Mechanics, The Johns Hopkins University, Baltimore, Maryland†

(Received 29 November 1966)

Laminar boundary layer on a flat plate with zero pressure gradient was excited by a solitary three-dimensional disturbance. The growth of the disturbance was studied using a 10-channel linearized d.c.-coupled hot-wire system. The development of the disturbance flow field was studied and compared with theory by Criminale & Kovasznay (1962). The experimental results indicate a departure from the theory on account of the simplifying assumptions made in the theory. Certain new results were also obtained.

1. Introduction

The stability of laminar shear flows and the transition to turbulent motion has received and continues to attract much attention because of the fundamental importance to the study of fluid motion. Even though considerable effort has been put into the study of transition, a complete understanding of the phenomenon has not been made. However, certain phases of the breakdown process have been clarified.

There is not even reasonable certainty that all flow configurations break down in the same manner. The breakdown mechanism may depend on the constrainment of the flow. The three different kinds of flows usually studied are: fully constrained (pipe flow, etc.), not constrained (free shear flow), and half constrained (boundary-layer flow). The greater part of the studies have been the investigation of breakdown process of a laminar boundary-layer flow on a flat plate.

On the theoretical side, the two-dimensional linearized theories have been well understood and their findings have been experimentally verified. The shortcoming of these theories is that they do not explain the mechanism of actual transition.

Emmons & Bryson (1952) observed the incipient turbulent spots on a water table and suggested the strongly three-dimensional nature of transition. Further experimental studies were concerned with these spots and their growth. These studies still did not answer how these turbulent spots originated, i.e. the development of instability that precedes them.

Klebanoff & Tidstrom (1959), Klebanoff, Tidstrom & Sargent (1962), Kovasz-

† Present address: Department of Aerospace Engineering, Pennsylvania State University.

nay, Komoda, & Vasudeva (1962) did extensive experiments exciting a laminar boundary layer using a vibrating ribbon. They have proved that the laminar instability waves are ultimately not two-dimensional but actually three-dimensional before transition actually occurs. The three-dimensional development of instability was also studied by Hama (1960) and Hama & Nutant (1963) using the dye technique and the hydrogen bubble technique and confirmed the importance of the three-dimensionality of the flow field before breakdown. However, the three results do not agree on some aspects of the phenomenon and hence it is not yet feasible to obtain a unified view of the transition process.

On the theoretical side, three-dimensional implications of linear instability were explored by Criminale & Kovasznay (1962). They calculated the fate of an isolated pulse-like disturbance in a laminar boundary layer with Blasius velocity profile. In order to study the growth and 'diffraction' of a spot-like disturbance, the initial disturbance was synthesized from all possible waves whose propagation velocities and amplification rates follow from the classical two-dimensional theory by Squire (1933). This initial disturbance was taken as circular Gaussian pulse.

During the initial period (solved explicitly) they found that there was a decrease in amplitude and the disturbance spread over a wide area. They also predicted the asymptotic behaviour which described the ultimate fate of the disturbance and the maximum rate of growth was found to vary as $(t^{-1}e^{t})$. They have shown that there is a gradual approach to the two-dimensional Tollmien–Schlichting wave train and this is seen as a wave packet, which spreads laterally as $t^{+\frac{1}{2}}$. The investigators have also shown that the vorticity due to the disturbance (circular Gaussian) velocity has only two components; one in the mean flow direction ω_x, and the other in the lateral direction, ω_z, and that in the initial period $\omega_x > \omega_z$, and at later times the inequality is reversed. Clearly all the three components of vorticity exist in the three-dimensional problem. However, for the particular type of disturbance assumed and the approximation used $\omega_y = 0$.

The experiments reported here are a logical extension of the work reported by Kovasznay, Komoda & Vasudeva (1962). The idea was to disturb the laminar boundary layer by a localized disturbance and to study the subsequent development both in its initial, linear phase and in the later highly non-linear range. The linearized problem has been treated earlier by Criminale & Kovasznay (1962) and the explicit predictions are available that will be checked against the results of the experiments reported here. The later, localized non-linear stage on the other hand will be compared with the breakdown pattern obtained earlier with the doubly periodic excitation (periodic in time and in the spanwise direction). If the results are in the affirmative we would find that the laminar instability is only creating a possible localized disturbance that further develops by non-linear amplification into a local spot of incipient turbulence, whose form does not depend on the laminar instability theory.

A partial list of symbols used throughout this article is given below:

x downstream direction parallel to free stream,

y direction normal to flat plate,

z spanwise direction,
x_0 location of disturbance generator,
U free-stream velocity,
u local mean velocity,
u' fluctuation velocity in the x-direction.

2. Equipment

The investigations were conducted in the 120×90 cm (48×36 in.) open return wind tunnel on an aluminium flat plate, 80 cm (32 in.) wide, 250 cm (96 in.) long and 0·55 cm (0·375 in.) thick with an asymetrically cut rounded leading edge.

Specially shaped fillers were placed in the corners to allow for the boundary-layer growth on the walls, and thus attain zero pressure gradient. The distribution of fillers along the corners was done by trial and error. The pressure gradient is shown in figure 1. All measurements were done at a free-stream speed of 760 cm/sec.

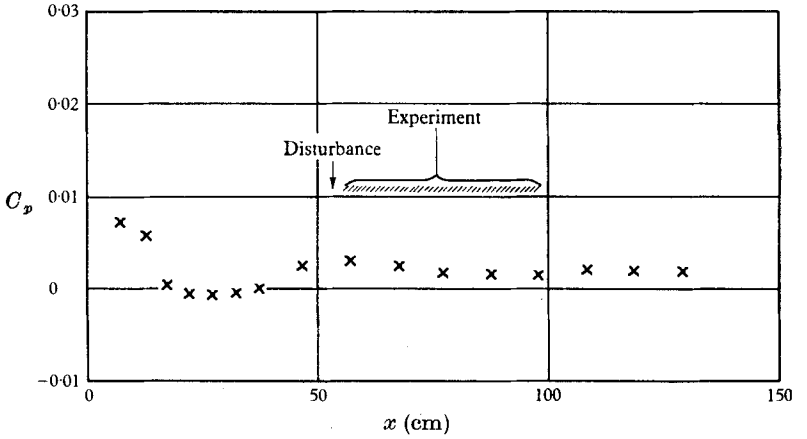

FIGURE 1. Pressure distribution on flat plate.

Boundary-layer profiles measured at different stations were indistinguishable from the Blasius profile. Boundary-layer thickness at $x = 58$ cm was 0·6 cm.

Reynolds number based on displacement thickness for the range of exploration was 900–1200. The curve of neutral stability for neutral frequencies of disturbances on a flat plate at zero incidence and the region of exploration is shown in figure 2.

Ten-channel transistorized and linearized constant temperature equipment built by the author was used. The equipment was developed earlier by Kovasznay, Miller & Vasudeva (1963).

The hot-wire probes were made of tungsten wires $3{\cdot}8 \times 10^{-4}$ cm (0·00015 in.) in diameter. The wires were first electroplated with copper, leaving a well-defined length bare, and then soft soldered to supporting prongs. Two lengths were used, 0·150 cm (0·060 in.) and 0·07 cm (0·028 in.).

Single wires placed normal to the mean flow were used for exploration or for obtaining a reference signal. Double probes consisting of two parallel wires were made for measurement of $\partial u/\partial y$ (the approximate vorticity component). The two wires were placed at a distance of 0·05 cm (0·020 in.), and the difference signal was regarded as approximate vorticity. The approximation amounted to the assumption that $\partial v/\partial x \ll \partial u/\partial y$. This approximation was later found to be in error in certain cases.

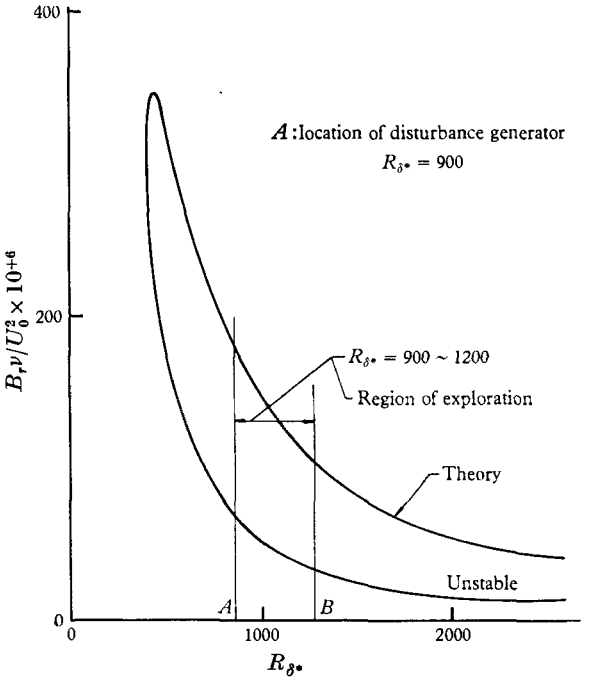

FIGURE 2. Curve of neutral stability.

In order to measure the instantaneous velocity distribution across the boundary layer, the 'ladder' hot-wires were placed 0·070 cm (0·028 in.) apart, forming an array to measure instantaneous velocity profiles.

For the simultaneous display of ten traces, no commercial equipment was available at reasonable cost. Therefore, a 10-channel display oscilloscope was built around a commercial television receiver (21 in. tube). The original horizontal (15 kc) scan was turned vertical, and was used as the basic vertical scan raster. The traces were displayed by pulse position modulation. The trace was formed by a series of dots on the screen that merged to continuous lines. Each channel had individual gain control, position control and intensity control. Since the input impedance of the channels was low, an intermediate buffer stage was put between the linearizer and the scope input. Thus, the linearizer 'looked' into a 100 K. impedance. The gain control and the position control were not independent. For visual observation a horizontal sweep was added, and the traces could also be synchronized to an external signal.

A Dumont oscilloscope camera was used to photograph the traces, with an auxiliary (negative meniscus) Kodak Telek. (-2) lens. For photographic recording the horizontal sweep was removed, and the vertical display was used. 100 ft. lengths of Kodak 35 mm Tri-X film (TX 417) were used in the camera. These films were developed in a continuously agitated developing tank. A speed of 20 in./sec was used.

Considerable effort was put into the design of the disturbance generator. The most important design feature of such a generator was that the type of disturbance (whatever it may be) should repeat event after event. Secondly, the amplitude of the disturbance should be adjustable so that the disturbance would not trip the boundary layer at the point of generation. Figure 3 shows the detailed construction of this disturbance generator.

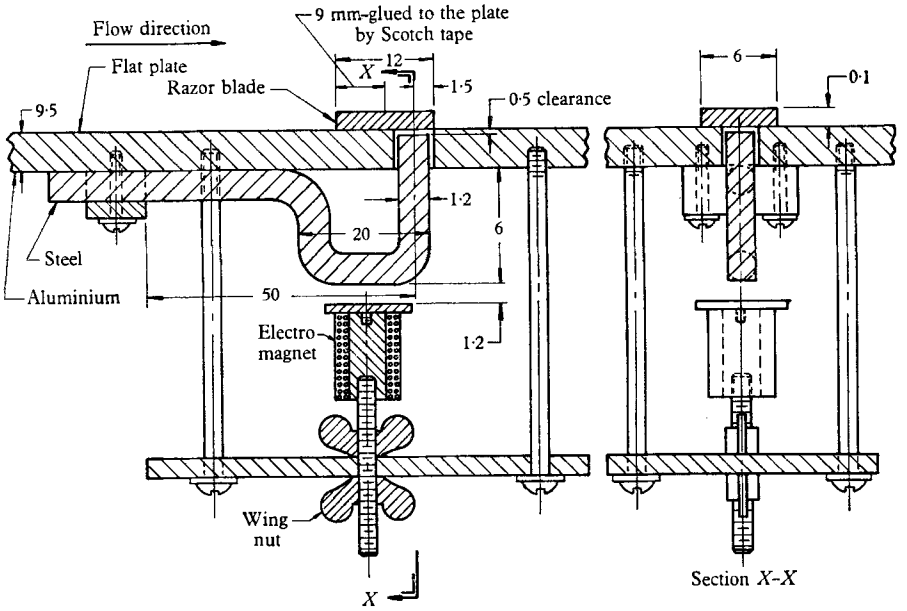

FIGURE 3. Disturbance generator. Note: drawing not to scale; only relevant dimensions shown; all dimensions in mm.

A brass plug 2·5 cm (1·0 in.) in diameter was screwed into the flat plate so that the plug was flush with the surface of the plate. A 0·15 cm diameter (0·06 in.) circular hole was drilled through the plug at the centre. A relay magnet was mounted at a distance of 0·72 cm (0·28 in.) from the back of the working side of the plate. This magnet was on a tripod, which was attached to the plate. It was possible to adjust the position of the magnet relative to the flat plate. The centre line of the magnet and the centre line of the hole in the plug were offset by 0·8 cm (0·32 in.).

A 7·5 cm (2·75 in.) length of piano wire, diameter 0·12 cm (0·5 in.) was taken and bent into the shape shown in figure 3. The 1·25 cm (0·5 in.) free portion of the wire (henceforth referred to as 'plunger') was inserted into the hole in the plug from the back side of the plate, and the longer free end of the wire was

clamped at its end to the flat plate. The 3·2 cm long (1·25 in.) length was straight and was flush with the surface of the plate. The free end of the piano wire, which was sliding through the hole, was not flush with the surface of the plate, but a little shorter. It was possible to adjust this distance.

When the electromagnet was supplied with power, the magnet would pull the piano wire. When the current was shut off it would release the wire, and the plunger would overshoot its equilibrium position and project slightly out of the surface of the plate. The distance between the magnet and the plunger, and the clearance between the surface of the plate and the free end of the plunger, was so adjusted that the plunger would rise above the surface of the plate only once during the first cycle of oscillations.

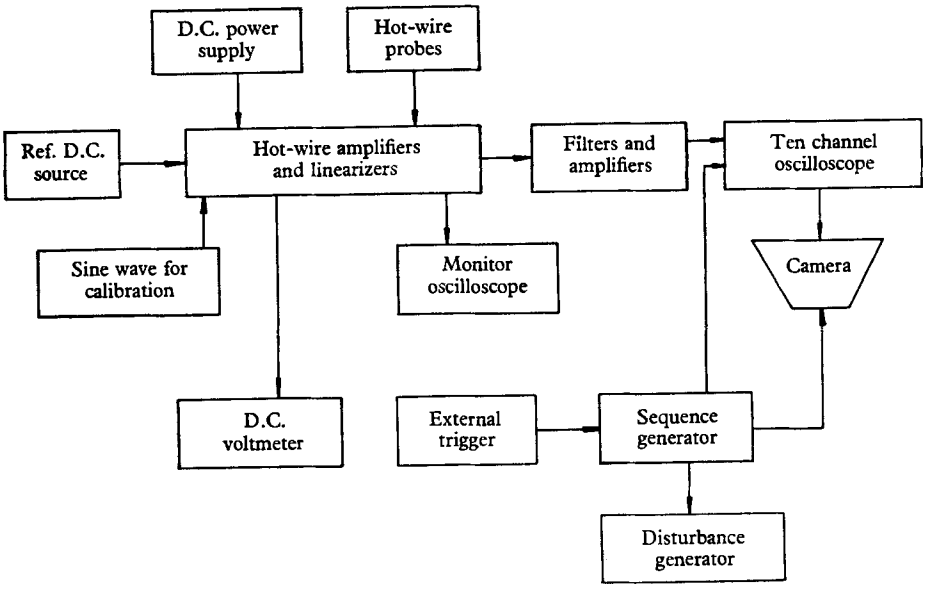

FIGURE 4. Block diagram of the experimental set up.

On the working side of the plate the 0·15 cm diameter circular hole on the brass plug was covered with a thin piece of razor blade, 1·2 × 0·6 cm (0·5 in. × 0·25 in.). The 1·2 cm side was placed parallel to the direction of the flow, and the 0·6 cm side was placed normal to the direction of the flow. A small part (0·9 cm (0·35 in.)) of the razor blade was taped to the plate, which left a 0·3 cm (0·12 in.) length free. The centre of this 0·3 cm free length coincided with the centre of the hole, and when the plunger was released from the magnet, the free end of the blade deflected. Since the plunger would not hit a second time, the free end of the blade would deflect only once. The amount of deflexion was adjustable by moving the position of the magnet relative to the flat plate.

If the free end of the blade was lifted up and a spacer (thickness equal to maximum deflexion of the blade) put below it, the flow would not be disturbed. Only the rapid movement of the free end of the blade would cause a disturbance in the flow. The actual aerodynamic disturbance caused consisted of two parts. One was the vortices shed from the free end of the blade, and the other was a thin

jet of air issued when the free end of the blade flapped back. The disturbance created by this above-mentioned disturbance generator was found to be very suitable, and the disturbance pattern was quite repetitive. A block diagram of the experimental set-up is shown in figure 4.

Several operational amplifiers (Philbrick G.A.P. Model K2/W) were used as single-shot multivibrators to provide a sequence of operation. The required sequence was as follows: the recording camera should attain constant speed. Next, the disturbance generator should be triggered. The outputs of the hot-wire probes should be recorded on the film in the camera, and the camera should then stop. This sequence was achieved by use of the operational set-up shown in figure 5.

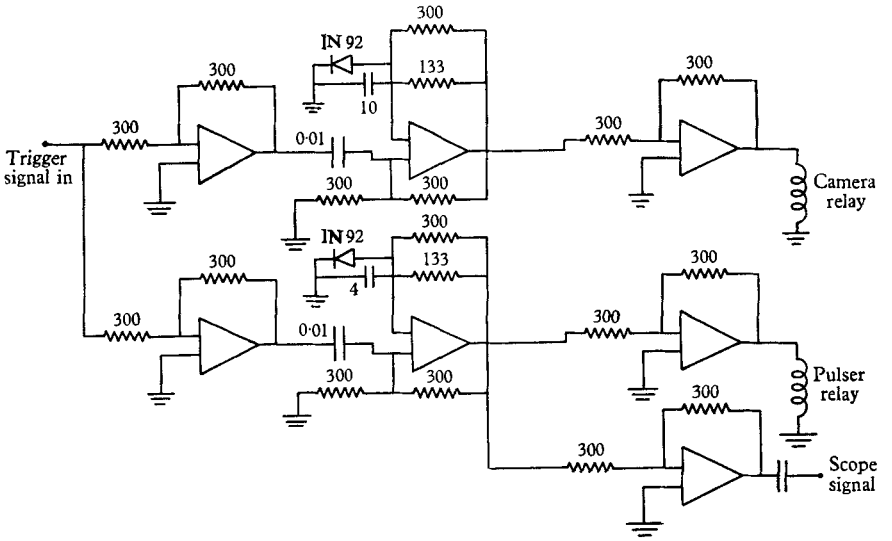

FIGURE 5. Operational amplifier set up for sequence generator. Note: operational amplifier Philbrick G.A.P. Model K2/W; Relay-Potter Bromfield 2500 SL; resistors, kilo ohms; capacitors, microfarads.

The electromagnet used in the disturbance generator was supplied by a 90-volt d.c. source. When the switch in the electromagnet circuit was closed, a pulse would activate a single-shot multivibrator. This, in turn, would activate a relay for 1 sec. The relay contacts formed the power switch for the recording camera. Thus, the camera would run for 1 sec. At the same time, the pulse which triggered the above single-shot multivibrator would also activate a second single-shot multivibrator, which would operate a second relay for 0·3 sec. The relay contacts were connected parallel to the power switch contacts in the electromagnet circuit. When the power switch was momentarily closed and then opened, this second relay would take over and break the electromagnet circuit after 0·3 sec. When the circuit was broken and the disturbance generator activated, a signal would go to one of the channels in the 10-channel oscilloscope. The trace from this channel would show when the disturbance was created for time reference. The two single-shot multivibrators were isolated by buffer amplifiers from the relays. They were also isolated from each other by two more buffer amplifiers.

The u' fluctuations caused because of the three-dimensional disturbance created inside the boundary layer were small ($\sim 2\,\%\ U$ to $3\,\%\ U = 30$–45 mV). Thus, the output from the hot-wire probes had to be amplified. Before amplification, it was necessary to filter the d.c. component, since the d.c. level varied, and the a.c. component was small.

It was also necessary to filter the high frequency components of the hot-wire output. If the high frequency components were not filtered, they, too, would get amplified and the traces were no longer smooth. Since the film strip was put in

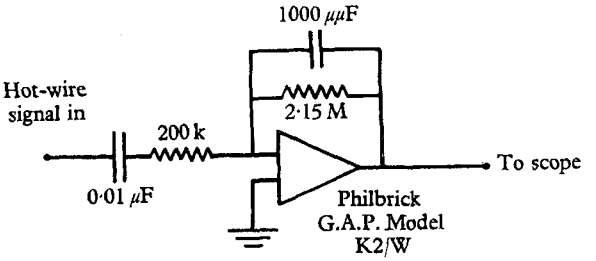

FIGURE 6. Filter and amplifier.

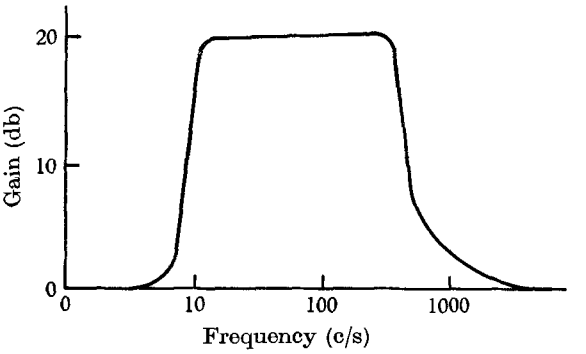

FIGURE 7. Gain characteristic of filter and amplifier.

an enlarger and traces copied on a graph sheet, it was difficult to achieve accuracy when copying. Since the phenomenon under investigation had frequency components well below 1000 cycles, frequencies above 1000 c/s were filtered. The amplification and the filtering of the hot-wire output was accomplished by the use of an operational amplifier (Philbrick G.A.P. Model K2/W) and proper capacitors. The circuit diagram is shown in figure 6. Since a one-stage amplifier was used, there was a 180° phase reversal. The gain characteristics of the filter and amplifier combination are shown in figure 7.

3. Experimental procedure

The 'ladder' probe and the double-wire probe, along with a single probe, were extensively used. When the 'ladder' probe was used, it was essential to know the exact distance between each wire. The geometrical distance between wires was not of much importance, but the effective aerodynamic distance was essential.

At a fixed station ($x-x_0 = 30$ cm), the 'ladder' probes were traversed across the boundary layer one after another (figure 8). The profiles were plotted on a graph sheet. From this, the effective aerodynamic distances between each wire could be estimated. The distance between wires was periodically checked. For the double-wire probe the same method was used to obtain the distance between

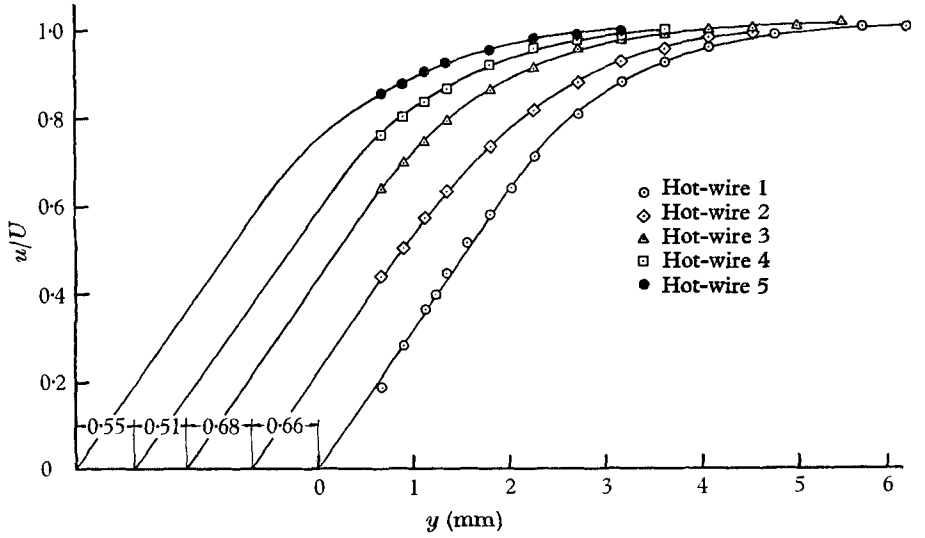

FIGURE 8. Boundary-layer traverse 'ladder' probe ($x-x_0 = 30$ cm).

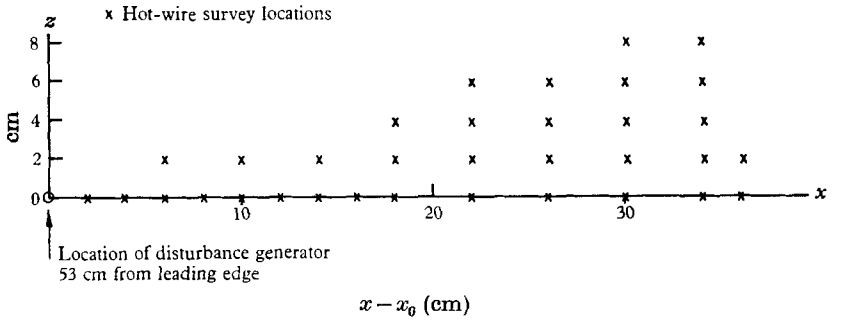

FIGURE 9. Hot-wire survey locations.

the two wires. The disturbance generator was situated at a distance of 53 cm (20·75 in.) from the leading edge. Free-stream velocity was 762 cm/sec (25 ft./sec). The 'ladder' probe and a $\partial u/\partial y$ probe were traversed at different stations. The stations surveyed are shown in figure 9.

Even though the disturbance created by the disturbance generator was identical each time, the u, $\partial u/\partial y$ output from the probes inside the boundary layer would differ because of the slow changes in the mean velocity in the free stream. Therefore, it was convenient to have a monitor probe at one fixed position inside the boundary layer. The output of this probe was always displayed on the 10-channel scope in addition to the output of the survey probes. The

monitor probe output then would serve as a reference, and it was used to select the proper sample of film. The location of the monitor probe was always at $x-x_0 = 54\,\text{cm}, z = 12\,\text{cm}, y = 0{\cdot}15\,\text{cm}$.

In the actual operation, the disturbance generator was pulsed five times, each pulse being a few seconds apart. It was necessary to take five shots for each position, as the free-stream velocity of the wind tunnel was varying. The 'ladder' probe then was moved to the next y position and the experiment repeated. To separate the five records from the following experiments, the last shot of each sequence was recorded without the 60 c/s time marker provided on the recording camera.

As mentioned before, a single-stage a.c. amplifier was introduced between the linearizer and the input to the 10-channel oscilloscope. To set the gain of the amplifier and the oscilloscope, a 40 mV r.m.s. 100 cycle sine wave was fed to the input of the amplifier. The gain of the amplifier was set previously. The gain of the oscilloscope was adjusted so that the sine wave was displayed between two reference lines displayed on the scope. To eliminate drift of the traces, the oscilloscope was turned on at least one hour before all adjustments were made.

4. Results

At each location, outputs from the 'ladder' hot-wire probe and the $\partial u/\partial y$ probe at different y locations were recorded on the film. For each y location the disturbance generator was triggered five times. It was possible to select the proper signal from these with few exceptions. The proper signals were selected by matching the output of the monitor probe.

One 'best' sample was chosen out of the five shots on the following basis: the desirable samples were those where the monitor probe showed well-defined sinusoidal wave 'packet' of a well-defined amplitude 15 mV. The sample was rejected, both if the disturbance was undeveloped (amplitude too small), or if the 'packet' had already broken down into a turbulent spot. This method assured that only the samples in the same stage of development were selected. There appeared to be a small, but irreducible, non-reproducibility in the high frequency details of the pulse. This is, of course, filtered out by the response of the boundary-layer disturbance amplification (rest of boundary layer can be regarded as a band-pass filter).

It was of prime importance to determine exactly at what time the disturbance was generated. This was possible by recording on the same film strip a signal that activated the disturbance generator. The time taken for the disturbance to arrive at a particular location could be easily determined from the film strip. It was interesting to note that when the monitor signal was matched for two or three records at the same location, the time of arrival also exactly matched, and when the monitor signals were different, the times varied too.

After determining the time of origin of the disturbance, it was possible to find the propagation velocity of the disturbance. It was relatively easy to determine the beginning of the disturbance within 0·5 ms, while the end of the distur-

bance could only be determined within 5 msec. One could see from the traces that the propagation velocity of the disturbance was different at different y locations. This will be discussed later. Even though the velocity of propagation was different, it was possible to determine the average time of arrival at a certain location. Figure 10 shows the time taken for the disturbance to arrive at each distance from the disturbance generator. From this figure, it can be seen that the velocity

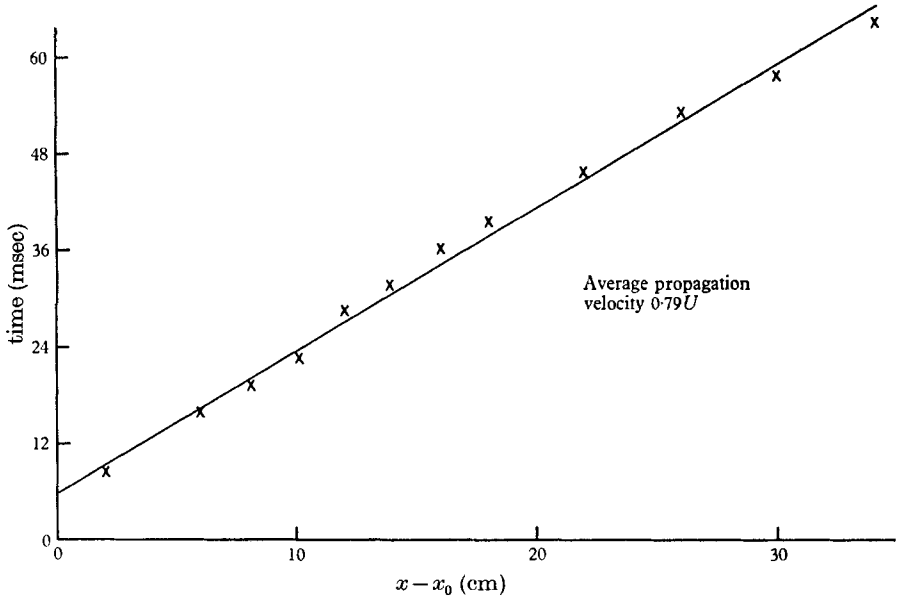

FIGURE 10. Time of arrival of disturbance.

of propagation is approximately constant, and is about $0{\cdot}8U$. This is quite a high value compared to the velocity of the Tollmien–Schlichting instability wave ($0{\cdot}37U$). However, Schubauer & Klebanoff (1955) have determined the propagation velocity of the front of a turbulent spot, and have arrived at a velocity of propagation of $0{\cdot}88U$. This is quite close to the $0{\cdot}8U$ measured by the author.

The propagation velocity of the end of the disturbance was computed for the present experiment as $0{\cdot}6U$. Schubauer & Klebanoff (1955) have determined the propagation velocity of the trailing end of a turbulent spot as $0{\cdot}5U$.

It can also be seen from figure 10 that the line drawn through the points on the graph does not pass through the origin. This can only be due to the fact that the virtual time origin of the disturbances differs from the time of triggering. Since the actual mechanism by which the disturbance was created was not well known, this off-set was not corrected, but all times were measured exactly in the same manner. It did not cause any serious problems, as time measurements were only relative to the nominal origin of the disturbance.

The actual u' fluctuations from the hot-wire probes were small, and so were amplified. The d.c. component was blocked before amplification, but the d.c. level was monitored separately. From a study of the signals it was possible to

determine crude maps of instantaneous flow field. The u' velocity increased and then decreased, crossed zero, further decreased, and then increased and crossed zero again. The differences in the characteristics of the various signals were the number of loops in each 'packet', and the time between zero crossings. Depending on the even or odd number of zero crossings, u' returned to zero at the end of the 'packet' from negative or from positive values.

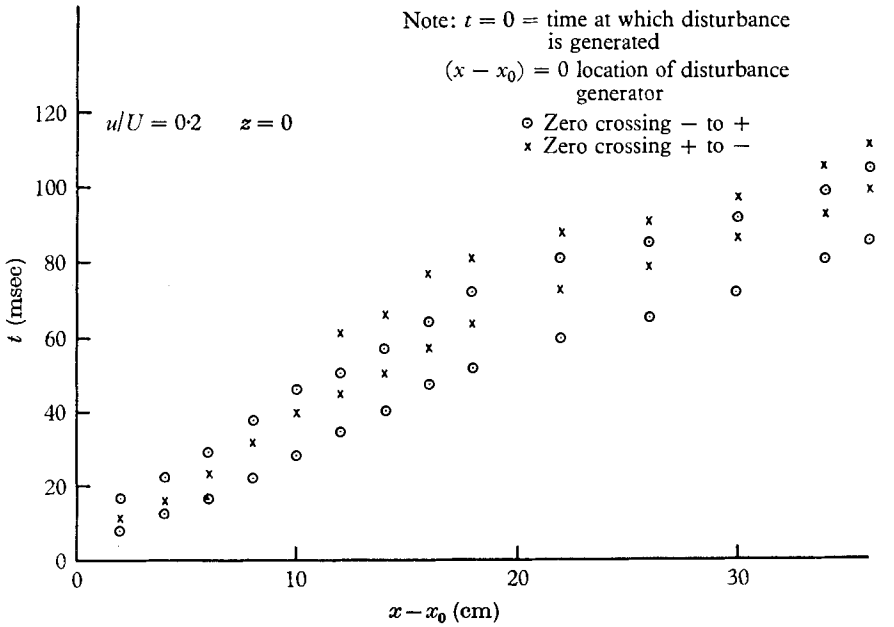

FIGURE 11. Zero crossing of u' fluctuations $u/U = 0{\cdot}2$; $z = 0$.

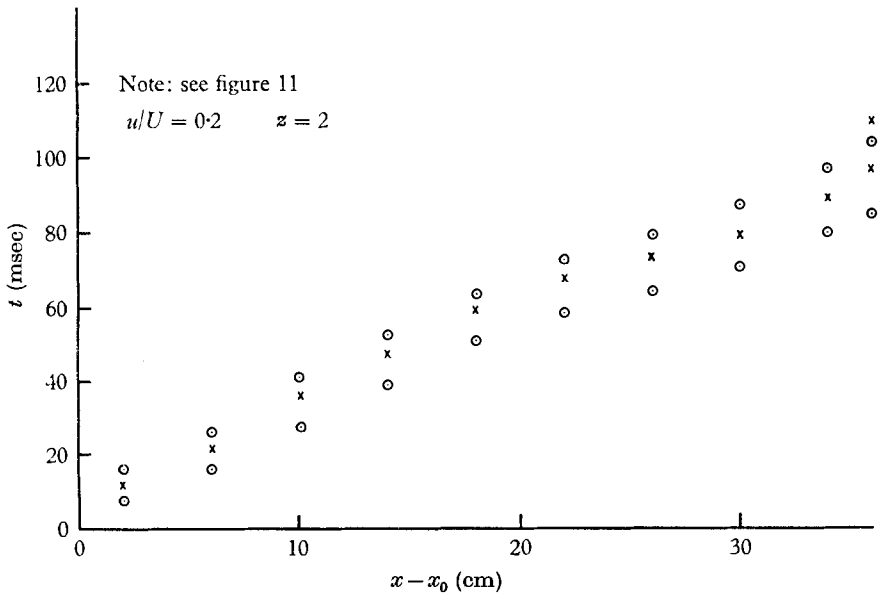

FIGURE 12. Zero crossing of u' fluctuations $u/U = 0{\cdot}2$; $z = 2$.

A zero crossing of the u' fluctuation for a particular y location was identified with an $x-x_0$ (survey location), and t ($t = 0$, origin of disturbance). For all survey locations a graph of y *vs.* t was plotted. There were two types of zero crossings. One occurred when the u' velocity went from negative to positive. The other occurred when the signal went through zero from positive to negative. The first departure from the mean value was always selected as the first zero crossing.

From such plots as described above, the following phenomenon was noticed. There was a variation in the time taken for the disturbance to arrive at different

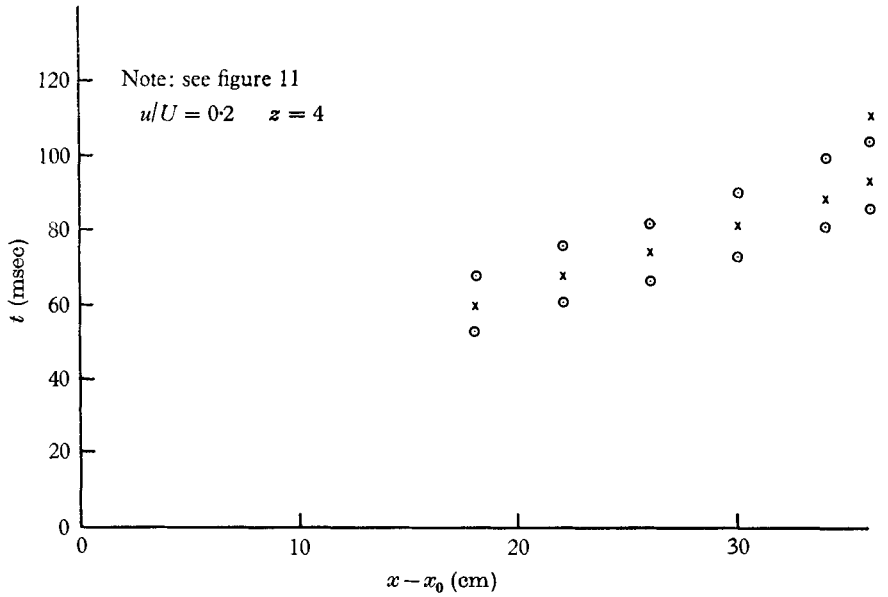

FIGURE 13. Zero crossing of u' fluctuations $u/U = 0{\cdot}2$; $z = 4$.

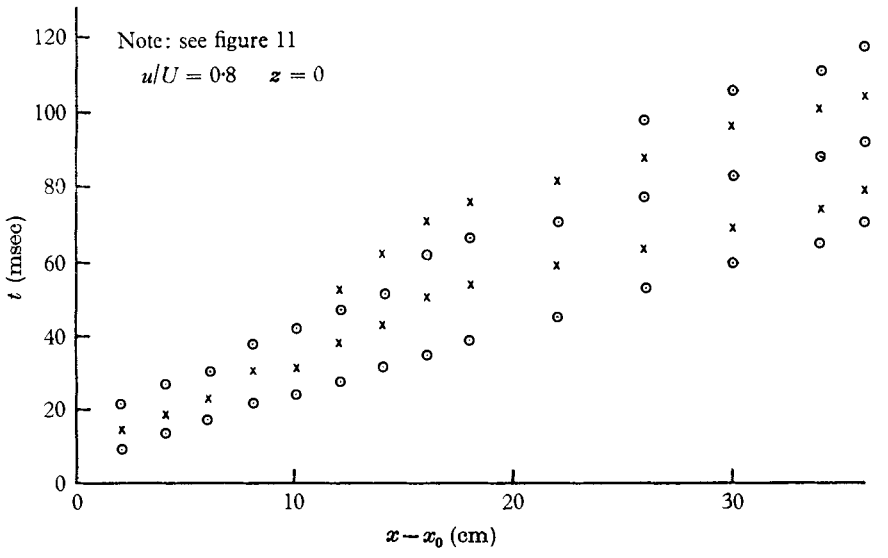

FIGURE 14. Zero crossing of u' fluctuations $u/U = 0{\cdot}4$; $z = 0$.

y positions. The disturbance arrived earlier far from the wall, and later closer to the wall.

At locations closer to the disturbance generator, the disturbances arrived at practically the same time. When the disturbances travelled downstream, the different time of arrival closer to the wall and near the free stream became apparent. The difference in time slowly increased but a change of character is observed around 18–20 cm.

As we have four independent variables (x, y, z, t), one must consider the variation with respect to each one of these. The variation with respect to y has been described above, and it shows a faster movement the further the distance from

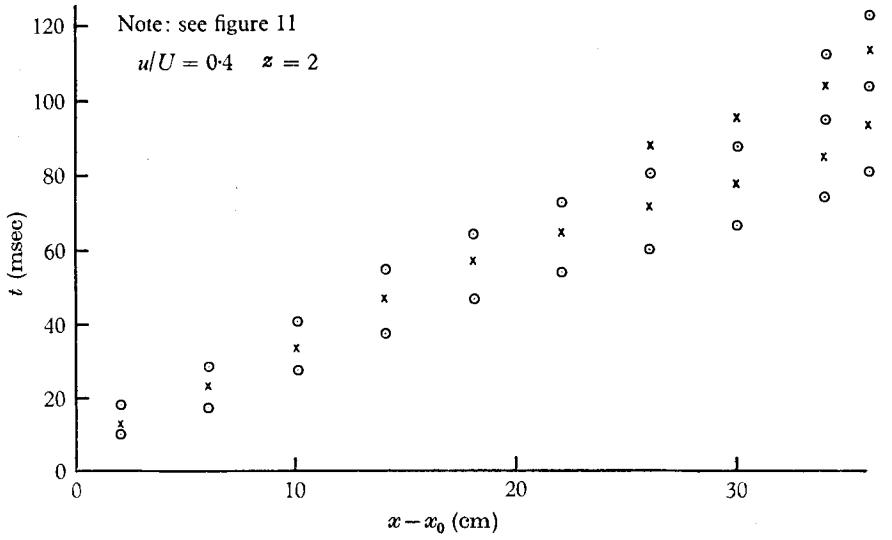

FIGURE 15. Zero crossing of u' fluctuations $u/U = 0{\cdot}4$; $z = 2$.

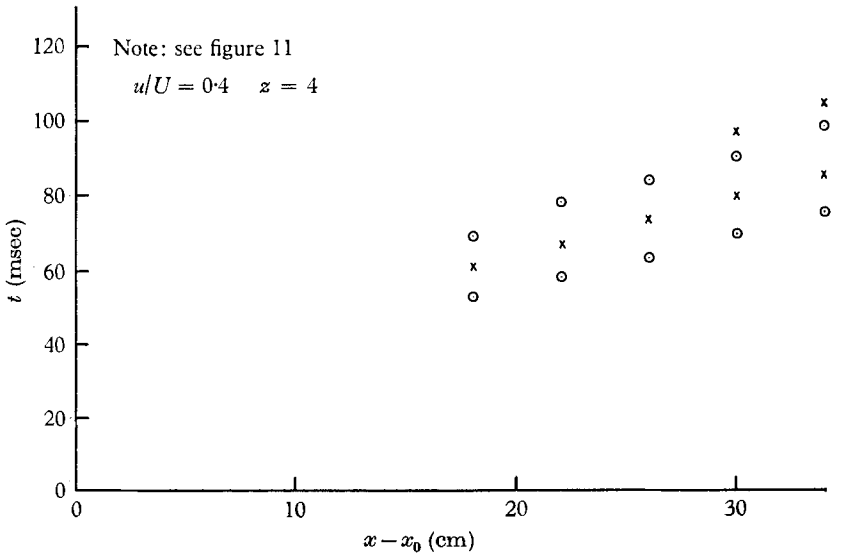

FIGURE 16. Zero crossing of u' fluctuations $u/U = 0{\cdot}4$; $z = 4$.

the wall. In the subsequent graph the distance from the wall is kept constant. As the boundary layer slightly increases in thickness (0·6–0·7 cm), it is more convenient to keep u/U = const. (The values of 0·2, 0·4, 0·8 were chosen.) For a given u/U, a plot of zero crossings is drawn on an (x, t)-plane. These plots are shown in figures 11–19 inclusive, for different values of u/U and of z.

Another plot gives the zero crossings on the (x, z)-plane at a constant value of u/U and at fixed time $t = 80$ ms. Figure 20 shows the different propagation velocities of the zero crossings at different u/U levels, and also the curvature of the wave front. It is evident from the figure that the zero crossing lines which are

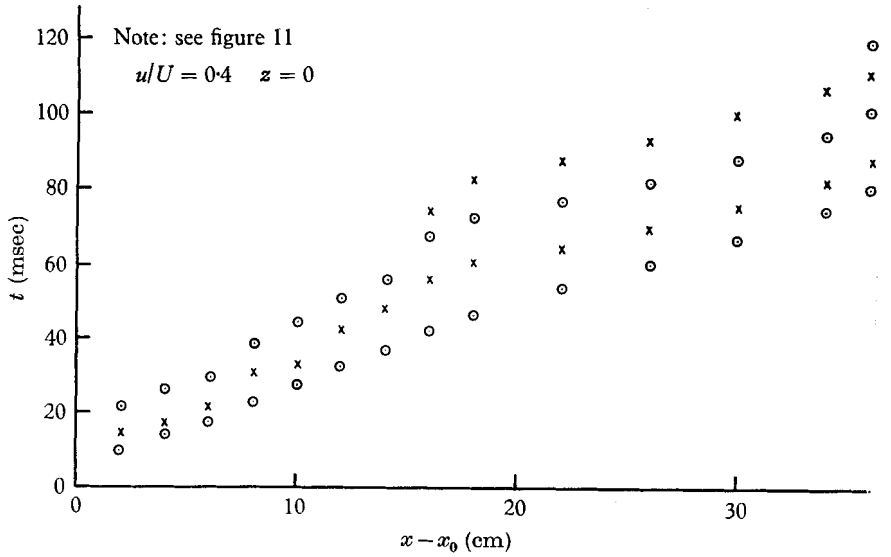

FIGURE 17. Zero crossing of u' fluctuations $u/U = 0{\cdot}8$; $z = 0$.

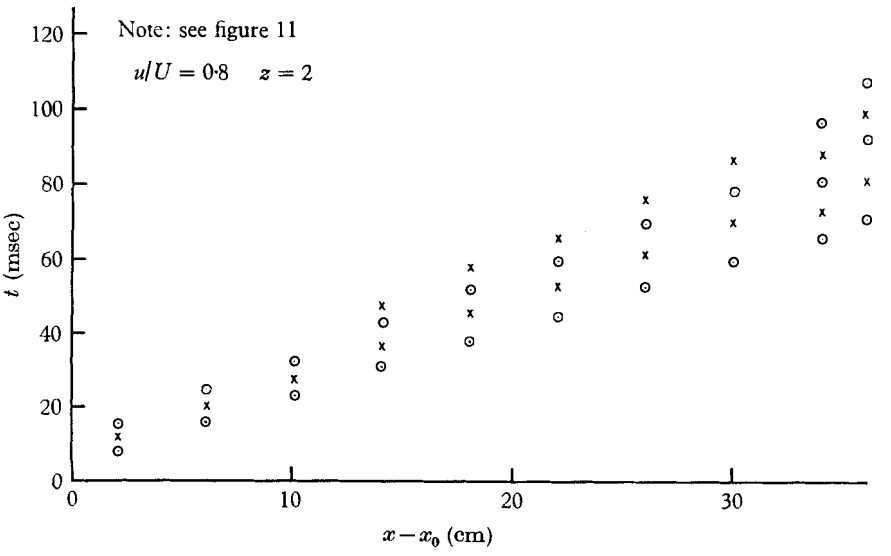

FIGURE 18. Zero crossing of u' fluctuations $u/U = 0{\cdot}8$; $z = 2$.

swept-back more at closer distances from the disturbance generator are straightened out further away from the plate.

The maximum u' fluctuation of the instability wave at $x-x_0 = 36$ cm was 3 % free-stream velocity. This amplitude, of course, decreases as z increases. At $x-x_0 = 36$ cm, $z \simeq 12$ cm, the flow was undisturbed.

Present experimental work was largely stimulated by the theoretical results of Criminale & Kovasznay (1962). In order to bring out the relationship, two special forms of presentation were chosen.

In one the instantaneous flow pattern was reconstructed. The time chosen was $t = 80$ ms. Essentially three things were needed: first, the location of the

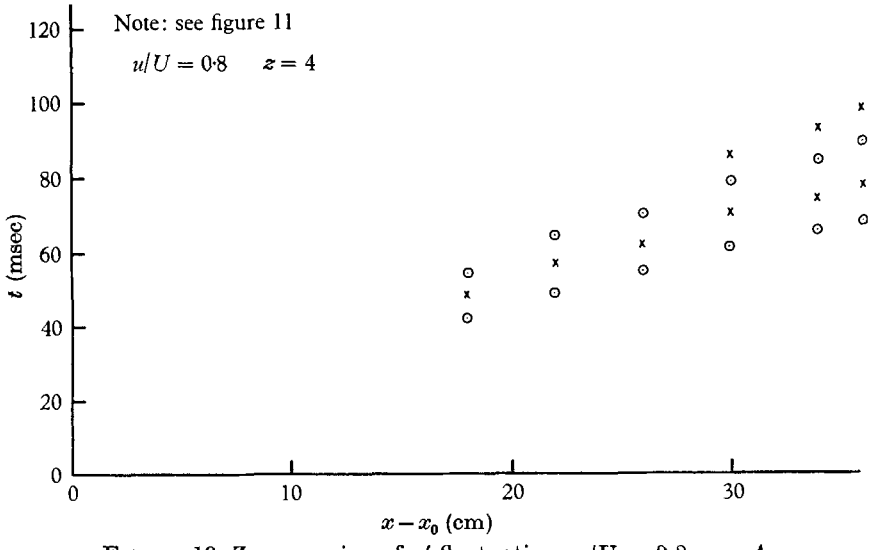

FIGURE 19. Zero crossing of u' fluctuations $u/U = 0{\cdot}8$; $z = 4$.

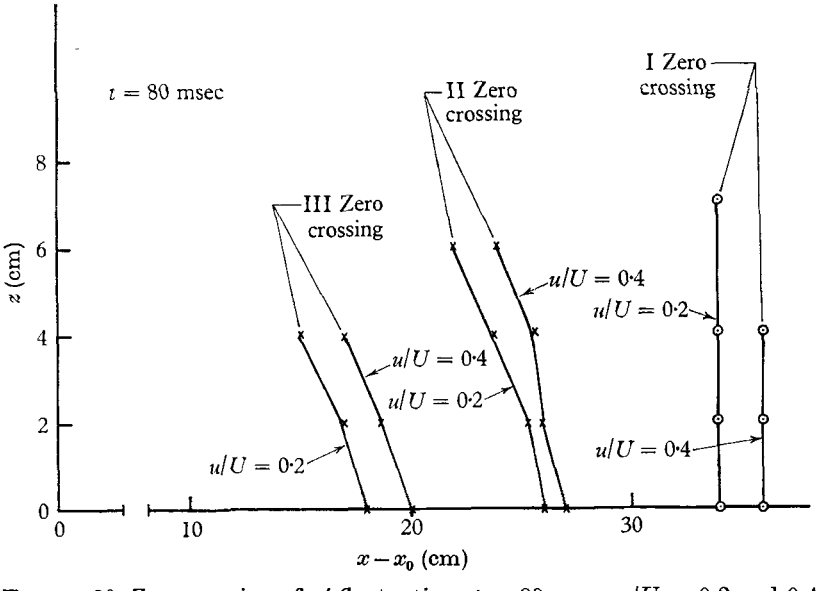

FIGURE 20. Zero crossing of u' fluctuations $t = 80$ msec, $u/U = 0{\cdot}2$ and $0{\cdot}4$.

zero crossings of the disturbance; secondly, the locations and magnitudes of the maximum amplitude 'ridges'; thirdly, the actual contour of constant u' interpolation between zero crossing lines and maximum 'ridges'.

The locus of zero crossings on the (x, z)-plane was determined as follows. From figures 11 to 19 inclusive, continuous traces were available for the movement of zero crossings. Cross-plotting these at t = const. gave the needed curves.

The 'ridges' of maximum and minimum were assumed to be half-way between the zero crossings (the traces indicate that this is a reasonable approximation). The amplitude values along the 'ridges' were determined by using auxiliary plots (separate for each z and u/U value) (not included) of values of maximum

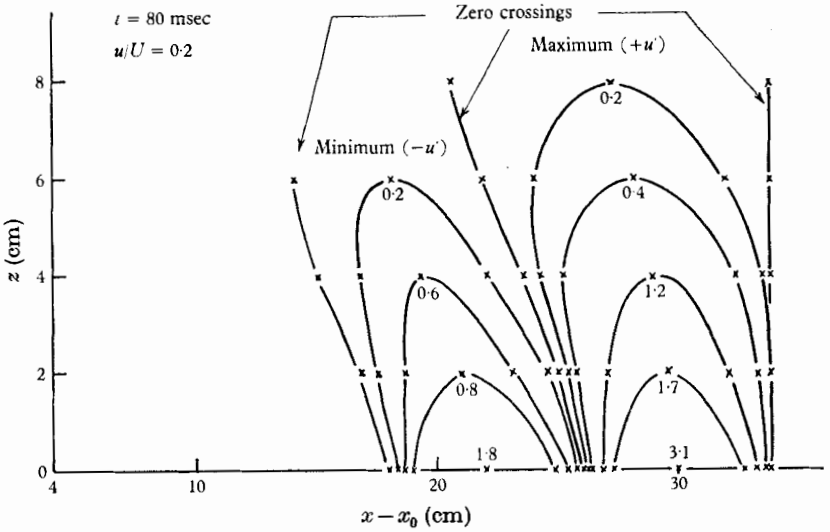

FIGURE 21. Reconstructed instantaneous flow field t = 80 msec, u/U = 0·2.

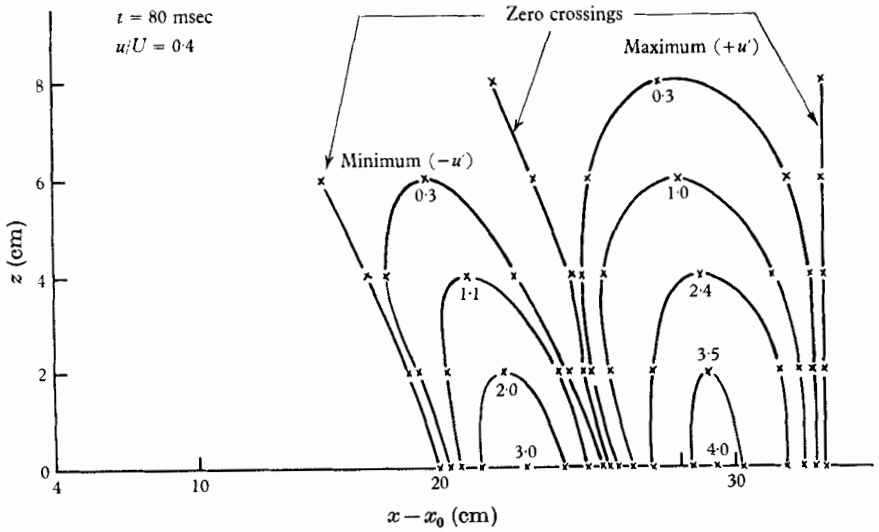

FIGURE 22. Reconstructed instantaneous flow field t = 80 msec, u/U = 0·4.

(and minimum) as a function of x. Using the approximate location of the 'ridges' the proper x values were read and the peak of the maximum cross plotted against z separately for each 'ridge'. From these the actual kidney-shape contours were drawn (figures 21 and 22).

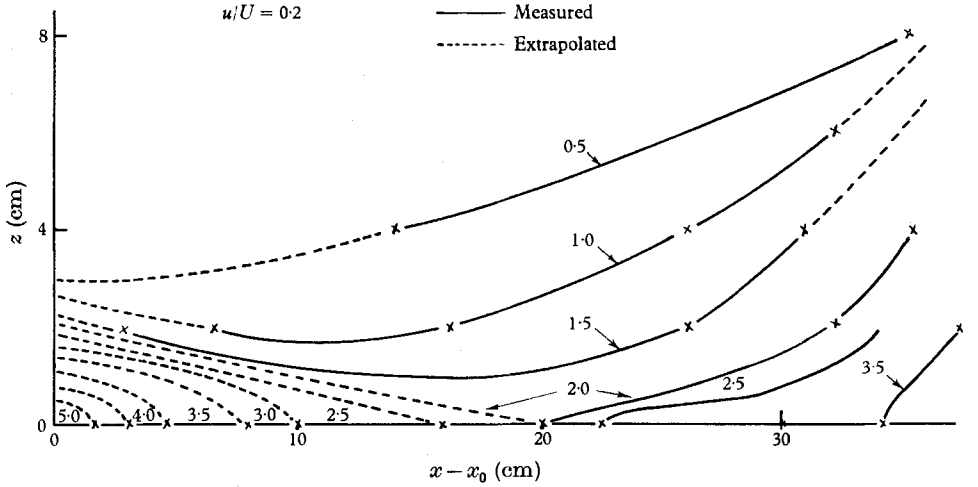

FIGURE 23. Maximum amplitude ever attained $u/U = 0{\cdot}2$

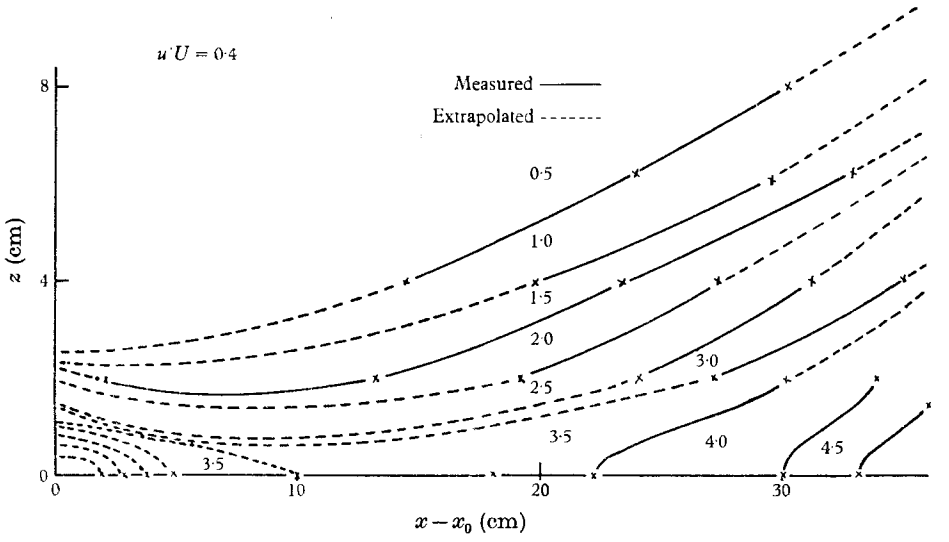

FIGURE 24. Maximum amplitude ever attained $u/U = 0{\cdot}4$.

Contours of 'maximum amplitudes ever' were obtained in the same manner as for the theoretically calculated solution in figure 14 of Criminale & Kovasznay (1962). At each observation point $(x, z, u/U)$ the maximum value of the u' 'ever' was only recorded and the contours of $(u/U)_{\max}$ drawn and given in figures 23 and 24 for three values of u/U.

5. Conclusion

The comparison with theory is best brought out in figures 21–4. The instantaneous flow pattern, of course, referred to u', while in the theory the v (normal) component was plotted. In the theory, an important assumption was made, namely, the variations of the flow pattern with respect to y were suppressed by assuming similarity of the pattern at all levels (equivalent membrane problem). The experimental results clearly show a systematic variation from the distance of the plate. The disturbances appear to move faster as one moves away from the plate, so the forward point of the disturbance is likely to be in the outer region of the boundary layer.

The contour of maximum amplitude ever attained clearly shows the saddle point predicted by the theory. The localized pulse-like disturbance first reduces in amplitude because of the selective amplification of the lower wave-number components, but also strong attenuation of the high wave-number components that are responsible for the pulse amplitude takes place. Later, however, the exponential growth of the most amplified wave-number takes over beyond the saddle-point.

The inclination of contours on the (x,z)-plane varies with altitude (u/U), but the general character is similar to the one in figure 12 of Criminale & Kovasznay (1962). The overall conclusion is that the general character of the calculated disturbances has been confirmed, while the experiment has shed light on the difference due to simplifying assumption, namely, the disturbance pattern is similar all across the boundary layer.

The author performed these investigations while working for the degree of Ph.D. at the Johns Hopkins University and wishes to thank his advisor Dr L. S. G. Kovasznay for his advice and encouragement throughout. This work was sponsored by project SQUID which is supported by the Office of Naval Research Department of the Navy.

REFERENCES

Criminale, W. O. & Kovasznay, L. S. G. 1962 *J. Fluid Mech.* **14**, 59–80.

Emmons, H. W. & Bryson, A. 1952 *Proc. First U.S. National Congress on Applied Mechanics*, pp. 859–868.

Hama, F. R. 1960 *Proc. of* 1960 *Heat Transfer and Fluid Mechanics Inst.* pp. 92–103.

Hama, F. R. & Nutant, J. 1963 *Proc. of* 1963 *Heat Transfer and Fluid Mechanics Inst.* pp. 77–87.

Klebanoff, P. S. & Tidstrom, K. D. 1959 *NASA TN* D-195.

Klebanoff, P. S., Tidstrom, K. D. & Sargent, L. H. 1962 *J. Fluid Mech.* **12**, 1–32.

Kovasznay, L. S. G., Komoda, H. & Vasudeva, B. R. 1962 *Proc. of* 1962 *Heat Transfer and Fluid Mechanics Inst.* pp. 1–26.

Kovasznay, L. S. G., Miller, L. T. & Vasudeva, B. R. 1963 *Project Squid, Technical Report* JHU-22-P.

Schubauer, G. B. & Klebanoff, P. S. 1955 *NACA TN*-3489.

Squire, H. B. 1933 *Proc. Roy. Soc.* A **142**.